Quarkonium production at the LHC: a data-driven analysis of NRQCD's predictions

Pietro Faccioli[a,b,*], Mariana Araújo[a,c], Valentin Knünz[c], Ilse Krätschmer[d], Carlos Lourenço[c,*], João Seixas[a,b]

[a] *Physics Department, Instituto Superior Técnico (IST), Lisbon, Portugal*
[b] *Laboratório de Instrumentação e Física Experimental de Partículas (LIP), Lisbon, Portugal*
[c] *European Organization for Nuclear Research (CERN), Geneva, Switzerland*
[d] *Institute of High Energy Physics (HEPHY), Vienna, Austria*

arXiv:1702.04208v1 [hep-ph] 14 Feb 2017

Abstract

While non-relativistic QCD (NRQCD) foresees a variety of elementary quarkonium production mechanisms naturally leading to state-dependent kinematic patterns, the LHC cross sections and polarization measurements reveal a remarkably simple production scenario, independent of the quantum numbers and masses of the quarkonia. Surprisingly, NRQCD is able to accommodate the observed universal scenario, through a series of conspiring cancellations smoothing out its otherwise variegated hierarchy of mechanisms. This seemingly unnatural solution implies that the χ_{c1} and χ_{c2} polarizations, not yet measured, are strong and opposite, representing the only potential exception to a remarkably simple picture of quarkonium production. The observation of a large difference between χ_{c2} and χ_{c1} polarizations, which cannot be indirectly extracted from existing measurements because they mutually cancel each other in their contribution to the observed J/ψ production, would be a smoking gun signal finally proving the multifaceted but mysteriously elusive structure of NRQCD. On the other hand, the measurement of two similar, small polarizations will urge improved P-wave calculations, if not a substantial revision of the NRQCD hierarchies.

Keywords: Quarkonium, Polarization, NRQCD, QCD, Hadron formation

1. Introduction

Non-relativistic quantum chromodynamics (NRQCD) [1] is generally considered as the best theory approach to study quarkonium production. It is important to compare its predictions to the experimental measurements recently made available by the LHC experiments, which already reach rather high quarkonium transverse momentum, $p_{\rm T} \approx 100\,{\rm GeV}$, where the calculations are expected to be more reliable. If discrepancies between the theory predictions and the measured patterns are found, it is crucial to investigate if those differences stem from problems in the conceptual foundations of the theory or from approximations and inaccuracies of the fixed-order perturbative calculations available at present.

In a previous publication [2], we considered the charmonium and bottomonium cross sections and polarizations measured at the LHC, in the mid-rapidity region, and brought to light their remarkably simple and universal patterns, when studied as a function of $p_{\rm T}/M$, where M is the quarkonium mass. We concluded that all the measurements can be remarkably well described simply assuming universal production and decay properties for the $^3{\rm S}_1$ and $^3{\rm P}_J$ quarkonia.

In this Letter we investigate if the simplicity of the existing measurements can be reproduced by the NRQCD theory, despite its complexity and its foreseen hierarchy of elementary mechanisms, as described in Section 3 of Ref. [2]; and, if so, in which specific conditions regarding the so-far unmeasured polarizations of the χ_{c1} and χ_{c2} P-wave mesons.

As in Ref. [2], we replace the calculated short-distance cross sections (SDCs) with parametrized functions fitted to the experimental data, to be compared only a posteriori with the corresponding perturbative calculations. We treat the direct χ_{c1}, χ_{c2} and ψ production cross sections as three freely and independently varying kinematic functions. However, in the absence of χ_c polarization measurements, we resort to calculated ingredients to fix them, according to two different scenarios, both inspired by NRQCD.

2. Data-driven NRQCD scenarios

We have shown in Ref. [2] (Fig. 6-left) a surprisingly good agreement between the fully data-driven shape of the unpolarized component of the cross section and that of the calculated NRQCD $^1{\rm S}_0^{[8]}$ SDC. While the "universal almost unpolarized" (UAU) scenario discussed there reflects the simplest explanation of the data patterns, the conjecture that χ and J/ψ productions are described by identical mixtures of the same unpolarized and polarized processes finds no correspondence in the hierarchies of the NRQCD factorization expansion, where, in particular, no significant contribution of the unpolarized $^1{\rm S}_0^{[8]}$ term is foreseen for χ production. In this Letter we consider a scenario capable of accommodating the NRQCD process hierarchies, using two different assumptions for the χ sector.

*Corresponding authors: pietro.faccioli@cern.ch, carlos.lourenco@cern.ch

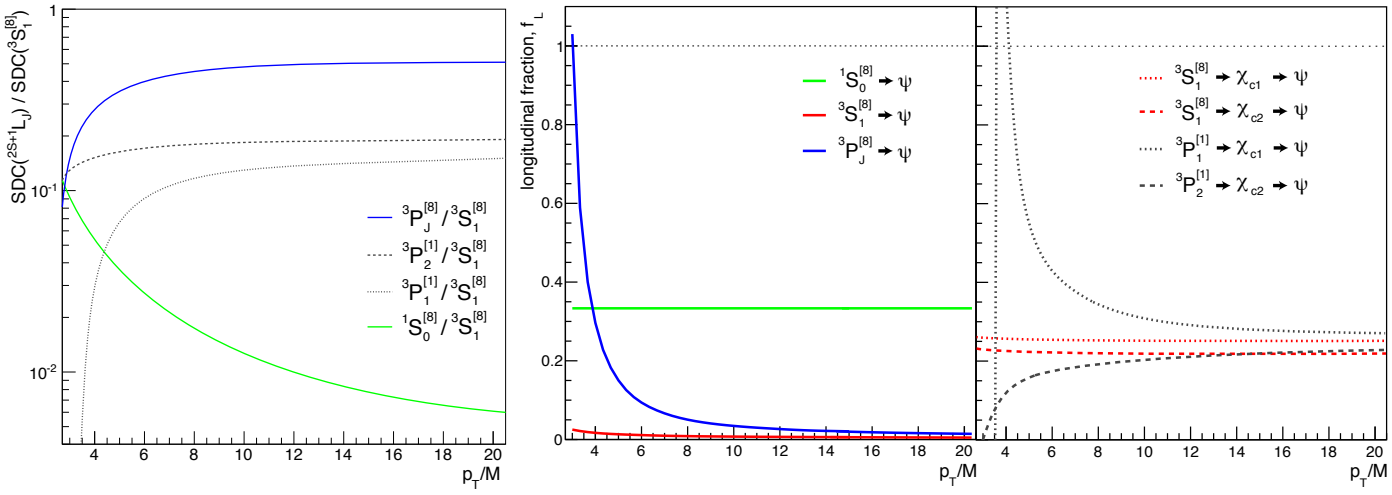

Figure 1: Comparison of SDC trends [3–5] as a function of p_T/M: SDC ratios with respect to the $^3S_1^{[8]}$ reference (left); longitudinal fractions for S-wave ("ψ") and P-wave ("χ") production (right). The $^3P_J^{[8]}$ and $^3P_{1,2}^{[1]}$ SDCs are multiplied by m_c^2, the squared charm-quark mass; they are negative and plotted with flipped signs.

Direct J/ψ production remains completely flexible and can accommodate any production scenario of non-longitudinal polarization. It is parametrized as a superposition of unpolarized and polarized processes, characterized, respectively, by $\lambda_\vartheta = 0$ and $\lambda_\vartheta = +1$, where λ_ϑ is the polar anisotropy parameter of the ψ dilepton decay. In more concrete terms,

$$\sigma_{\rm dir}(p_T/M) = \sigma^*_{\rm dir}[(1 - f^*_{\rm p})\, g_{\rm u}(p_T/M) + f^*_{\rm p}\, g_{\rm p}(p_T/M)] \,, \quad (1)$$

with $\sigma^*_{\rm dir}$ and $f^*_{\rm p}$ being, respectively, the total direct-production cross section and the fractional contribution of the polarized process, calculated at a reference point, set to $(p_T/M)^* = 2$ in our study. For $g_{\rm u}(p_T/M)$ and $g_{\rm p}(p_T/M)$, we take the empirical power-law functions defined in Eq. 5 of Ref. [2], normalized at $(p_T/M)^*$, determined by the corresponding shape parameters: β_u, β_p and a common γ (i.e., $\gamma_u \equiv \gamma_p$). The ψ(2S) is identically parametrized, with the same shape parameters and $f^*_{\rm p}$.

Given the absence of χ polarization measurements, the modelling of the direct χ_1 and χ_2 cross sections, instead, requires that we make a specific choice regarding these polarizations. This choice represents the only model-dependent ingredient of the analysis and the most substantial difference with respect to the UAU scenario, where we imposed that both χ_1 and χ_2 have identical process composition as for J/ψ production.

To maintain full generality, we model the χ_1 and χ_2 direct cross sections as two individual and independent functions, defined by two additional power-law shape parameters, β_{χ_1} and β_{χ_2}, while imposing the universal γ (i.e., $\gamma_{\chi_1} \equiv \gamma_{\chi_2} \equiv \gamma$). Therefore, we have a total of four independent and individually-observable cross-section contributions to quarkonium production: the unpolarized and polarized ψ terms, plus the χ_1 and χ_2 ones. Their hypothetical NRQCD counterparts are, respectively: $^1S_0^{[8]}$, $^3S_1^{[8]} + {}^3P_J^{[8]}$, $^3S_1^{[8]} + {}^3P_1^{[1]}$ and $^3S_1^{[8]} + {}^3P_2^{[1]}$.

We adopt two different χ polarization models. The first scenario, NRQCD 1, deliberately in line with the criterion of simplicity guiding our analysis, is inspired by some recurring trends in the NRQCD perturbative calculations of P-wave components, illustrated in Fig. 1: with increasing p_T/M the terms $^3P_J^{[8]}$, $^3P_1^{[1]}$ and $^3P_2^{[1]}$ become more and more indistinguishable from the $^3S_1^{[8]}$ term, in both cross section shapes and polarizations (or longitudinal fractions, $f_L = \sigma_L/(\sigma_T+\sigma_L)$, shown in the figure). This observation, also illustrated in Fig. 4 of Ref. [2], suggests an hypothetical theory scenario where, as the perturbative calculations improve, the three P-wave terms rectify their low-p_T behaviour, tending to assimilate their shape to the one of their "complementary" $^3S_1^{[8]}$ term. This conjecture justifies our first modelling of the unknown χ_1 and χ_2 polarizations: we assume them to be constant and equal to 1/5 and 21/73, respectively, therefore similar to one another and to the measured J/ψ and ψ(2S) polarizations, in perfect coherence with the observed universal patterns. These values are obtained with the relations

$$\begin{aligned} \lambda_\vartheta^{\chi_1} &= \lambda_\vartheta^{\rm J/\psi}/(4 + \lambda_\vartheta^{\rm J/\psi}) \,, \\ \lambda_\vartheta^{\chi_2} &= 21\lambda_\vartheta^{\rm J/\psi}/(60 + 13\lambda_\vartheta^{\rm J/\psi}) \,, \end{aligned} \quad (2)$$

when setting the decay anisotropy parameter of the J/ψ meson to $\lambda_\vartheta^{\rm J/\psi} = \lambda_\vartheta(^3S_1^{[8]}) = +1$.

The second scenario, NRQCD 2, uses genuine NRQCD χ_c polarization predictions, obtained including $^3P_{1,2}^{[1]}$ terms as currently calculated at NLO [3–5]. In NRQCD, the χ polarizations and the χ_2/χ_1 cross-section ratio are functions of one common parameter, equal for all χ_c states,

$$K_\chi = (1/m_c^2)\, \mathcal{L}_{\chi_{c0}}(^3P_0^{[1]})/\mathcal{L}_{\chi_{c0}}(^3S_1^{[8]}) \,, \quad (3)$$

where $\mathcal{L}$ denotes the long distance matrix element (LDME) and m_c^2 is the mass of the charm quark, squared. Because of heavy-quark spin-symmetry (HQSS), both the full χ_c production cross sections (σ_J, $J = 0, 1, 2$) and the "spin projections" (spin-density matrix elements) $\sigma_J^{00} \ldots \sigma_J^{JJ}$ used to calculate λ_ϑ have the general form

$$\sigma_J \propto (2J + 1)\left(m_c^2 \mathcal{S}(^3P_J^{[1]}) + K_\chi \mathcal{S}(^3S_1^{[8]})\right) \,, \quad (4)$$

where, in the case of a spin-projected cross section, $\mathcal{S}$ represents the corresponding spin-projected SDC. Using this equation to represent the numerator ($J = 2$) and denominator ($J = 1$)

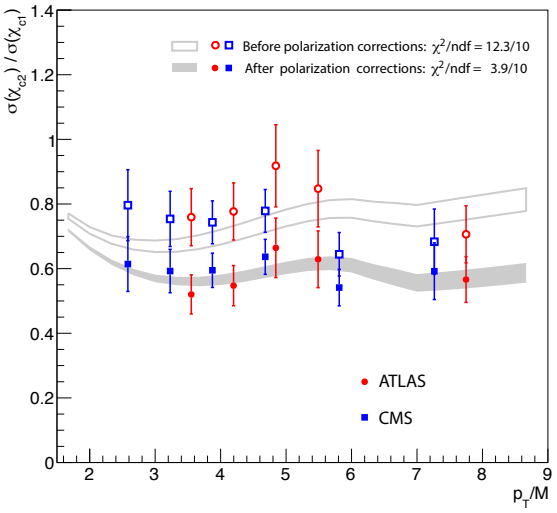

Figure 2: Fit of the χ_{c2}/χ_{c1} ratio measured by ATLAS [7] and CMS [8], before and after properly accounting for the dependence of the detection acceptances on the (simultaneously calculated) χ_1 and χ_2 polarizations. The filled markers are the data points acceptance-corrected according to the best-fit polarizations (shown in Fig. 3). The width of the best-fit band reflects the K_χ uncertainty.

of the χ_2/χ_1 ratio, we obtain 5/3 when the singlet contributions vanish ($K_\chi = 0$). The spin-density matrix elements [3–5] and λ_ϑ are related by

$$\lambda_\vartheta^{\chi_1} = (\sigma_1^{00} - \sigma_1^{11})/(\sigma_1^{00} + 3\sigma_1^{11}) \,,$$
$$\lambda_\vartheta^{\chi_2} = (-3\sigma_2^{00} - 3\sigma_2^{11} + 6\sigma_2^{22})/(5\sigma_2^{00} + 9\sigma_2^{11} + 6\sigma_2^{22}) \,, \quad (5)$$

where each of the spin-density matrix elements is a linear combination of the ${}^3P_J^{[1]}$ and ${}^3S_1^{[8]}$ terms, according to Eq. 4. This induces the λ_ϑ dependence on K_χ. It is important to note that, for what concerns the χ polarization parameters $\lambda_\vartheta(\chi_{1,2})$, we always refer to the corresponding dilepton decay distributions of J/ψ from χ. These are, in fact, the distributions that the experiments will measure directly and the ones needed to constrain the polarization of direct J/ψ production through a global analysis. Moreover, the dilepton decay parameters are identical to the $\chi \to J/\psi\,\gamma$ parameters, with the important advantage of being insensitive to the uncertain contributions of higher-order photon multipoles [6].

Leading-power fragmentation corrections have not yet been calculated for the ${}^3P_{1,2}^{[1]}$ singlets. Therefore, for consistency, we do not use, in Eq. 4, the available ${}^3S_1^{[8]}$ corrections [9] in the case of χ production.

We can determine K_χ from the measured χ_2/χ_1 ratio and then calculate the corresponding NRQCD polarization predictions. However, we must take into account that the χ_2/χ_1 ratio measurements strongly depend on the χ_1 and χ_2 polarizations assumed for the corrections of the detector's acceptance (phase space coverage). Therefore, for every K_χ value considered, we calculate the χ_1 and χ_2 polarization predictions and then correct the published ratio by the corresponding acceptance ratio. The corrected measurement is then compared (with statistical and systematic uncertainties, but without polarization uncertainties) with the prediction (for that K_χ value), to calculate the corresponding χ^2 value.

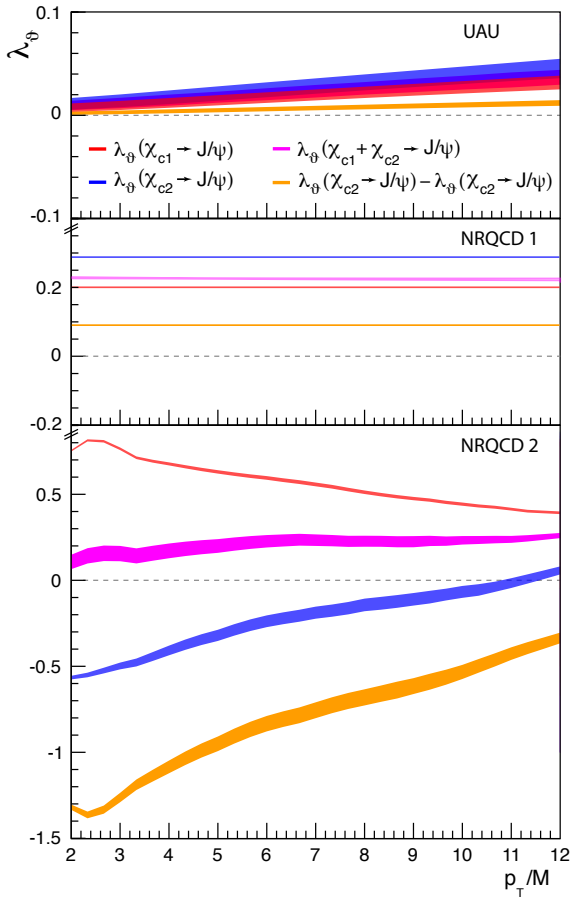

Figure 3: χ_{c1} and χ_{c2} polarizations as *fitted* in the UAU scenario (top), with bands reflecting correlated parameter variations, and as *assumed* in the NRQCD 1 (middle) and NRQCD 2 (bottom) scenarios. We also show the difference and the weighted sum (using the J/ψ feed-down contributions as weights) of the two polarization parameters. The NRQCD 1 constant lines reflect the hypothesis of ${}^3P_{1,2}^{[1]}$ polarizations assimilated to the ${}^3S_1^{[8]}$ polarizations, while the NRQCD 2 curves are weighted sums of the ${}^3S_1^{[8]}$ and ${}^3P_{1,2}^{[1]}$ polarizations, with weights resulting from fitting the χ_2/χ_1 data (Fig. 2).

Figure 2 shows how the χ_2/χ_1 ratio changes and the theoretical fit improves when we use the "proper" NRQCD polarization conjecture instead of the default unpolarized scenario that the experiments assume to report the central values of the measurements. The result of the fit is $K_\chi = 4.60 \pm 0.06$, a value only marginally consistent with the (much more uncertain) value assumed in Ref. [4] for the ${}^3P_J^{[1]} + {}^3S_1^{[8]}$ mixing parameter ($1/K_\chi = 0.27 \pm 0.06$, i.e. $K_\chi = 3.7^{+1.0}_{-0.7}$ in our definition). Their result reflects two incorrect ingredients: the use of the unpolarized acceptance scenario and the interpretation of the entire spectrum of polarization hypotheses as part of the experimental uncertainty.

The polarization predictions obtained with our K_χ value, and used as input to the NRQCD 2 scenario, are shown in Fig. 3. As p_T/M decreases, they tend to the extreme physical values $\lambda_\vartheta = +1$ and $-3/5$ for the χ_1 and χ_2, respectively. These maxima, while representing very different decay distributions, actually correspond to pure $J_z = 0$ alignment configurations of the two χ states, along an axis coinciding, in that limit, with

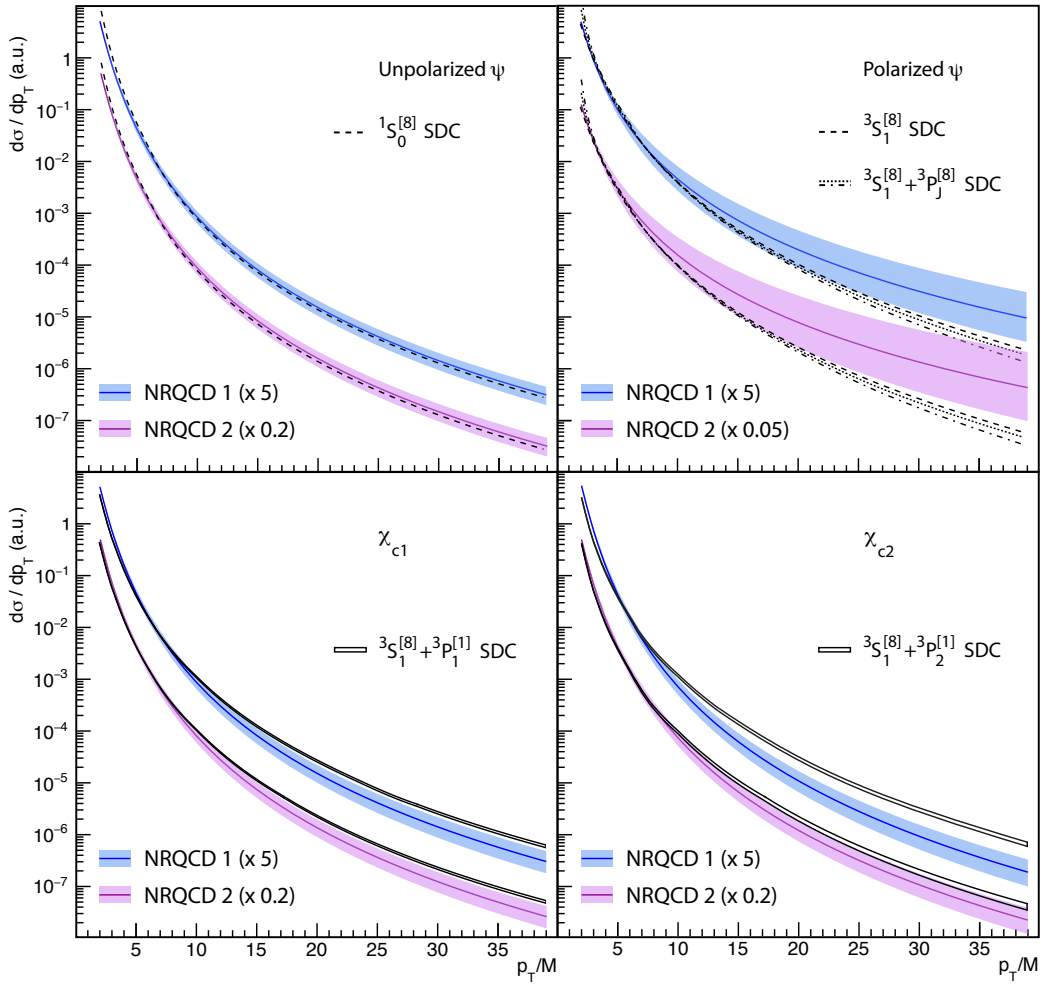

Figure 4: Cross section contributions (normalized to unity at $p_T/M = 2$) in the NRQCD 1 and NRQCD 2 scenarios, with uncertainty bands reflecting correlated variations in the fit parameters. The SDC combinations, arbitrarily normalized, are also shown (with band widths reflecting the K_χ values given in the text).

the direction of the colliding partons. Figure 3 also shows the constant polarizations used as inputs in the NRQCD 1 scenario and the predictions resulting from the UAU fit [2].

The NRQCD 1 and NRQCD 2 fits use the same data inputs as the UAU fit. Both best-fit results are very similar to those seen in Fig. 5 of Ref. [2]: the three scenarios describe the data very well, with almost identical minimum χ^2 values. The resulting shape parameters are, for the NRQCD 1 and NRQCD 2 fits, respectively:

$$\begin{aligned}
\gamma &= 0.74 \pm 0.20 \text{ and } 0.73 \pm 0.19 \,, \\
\beta_u &= 3.430 \pm 0.046 \text{ and } 3.421 \pm 0.045 \,, \\
\beta_p &= 2.78 \pm 0.22 \text{ and } 2.67 \pm 0.29 \,, \\
\beta_{\chi_1} &= 3.440 \pm 0.082 \text{ and } 3.458 \pm 0.082 \,, \\
\beta_{\chi_2} &= 3.54 \pm 0.10 \text{ and } 3.49 \pm 0.10 \,.
\end{aligned} \tag{6}$$

The corresponding polarized fractions, at $(p_T/M)^* = 2$, are $f_p^* = (1.8 \pm 1.5)\%$ and $(0.9 \pm 1.2)\%$.

The shapes of the cross-section terms obtained with the NRQCD 1 and NRQCD 2 fits are shown in Fig. 4, the data-driven bands being compared with the corresponding NRQCD SDC combinations. The unpolarized and polarized ψ panels show, respectively, the $^1S_0^{[8]}$ and $^3S_1^{[8]}$ SDCs, calculated at next-to-leading order (NLO) with fragmentation contributions [9]. The polarized panel also shows two curves representing a possible $^3P_J^{[8]}$ contribution added to the $^3S_1^{[8]}$ term, assuming $K_\psi = (1/m_c^2)\ \mathcal{L}_{J/\psi}(^3P_0^{[8]}) / \mathcal{L}_{J/\psi}(^3S_1^{[8]}) = 0.1$ and 0.2. Higher $^3P_J^{[8]}$ contributions lead to steeper curves, further departing from the fit result, which prefers the $^3S_1^{[8]}$ term alone. In fact, given the slight increase of the measured polarizations with increasing p_T/M, the data prefer a flatter polarized term than any $^3S_1^{[8]} + ^3P_J^{[8]}$ combination. Nevertheless, a residual $^3P_J^{[8]}$ contribution cannot be excluded, given the current experimental uncertainty; more precise polarization data, especially at high p_T/M, will make the comparison significantly more stringent.

Making specific hypotheses about the physical nature of the unpolarized and polarized contributions allows us to extract LDME values from the comparison with the calculated SDCs. For example, identifying the unpolarized cross section with the $^1S_0^{[8]}$ term, the corresponding LDME for a given state is

$$\mathcal{L}(^1S_0^{[8]}) = (1 - f_p)\, \sigma_{dir} / \mathcal{S}(^1S_0^{[8]}) \,. \tag{7}$$

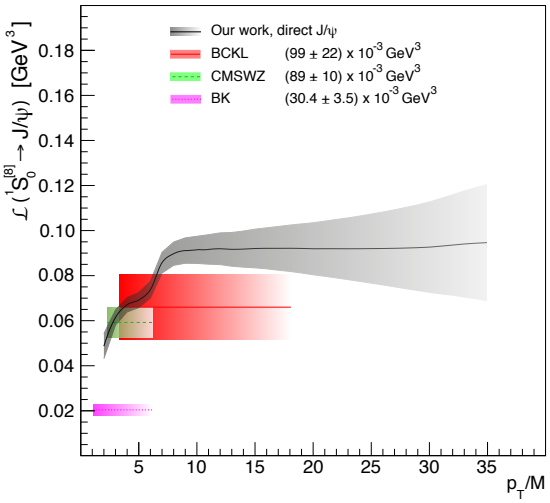

Figure 5: $^1S_0^{[8]}$ LDME for direct J/ψ production in the NRQCD 2 scenario (grey band), compared to results obtained in other analyses: BK [10], CMSWZ [3] and BCKL [9].

Using the SDCs calculated at NLO complemented with fragmentation contributions, for the production of a $Q\overline{Q}$ pair with 3 GeV of rest energy, the fit results for the *direct* J/ψ cross section in the NRQCD 2 scenario lead to the $^1S_0^{[8]}$ LDME represented by the grey band in Fig. 5. The width of the band only represents the experimental uncertainty; it does not reflect possible changes of the calculations due to scale dependencies (mostly a normalization shift) or to potential higher-order improvements.

As evident in the figure and implied by Eq. 7, where f_p, σ_{dir} and $\mathcal{S}(^1S_0^{[8]})$ are functions of p_T/M, the (supposedly constant) coefficient $\mathcal{L}(^1S_0^{[8]})$ becomes, technically, a function of p_T/M. This illustrates how the universality of the LDMEs, and hence the validity of the factorization hypothesis itself, are in reality only approximations relying on the goodness of the perturbative SDC calculations at a given order. The extracted LDME increases by a factor of 2 in the low-p_T/M region, presumably more affected by calculation uncertainties, and then stabilizes. Also for this reason, the LDME, when expressed by a constant number, necessarily depends on the method used for theory-data comparison. Figure 5 also shows the $\mathcal{L}(^1S_0^{[8]})$ results obtained in three different analyses of charmonium production, CMSWZ [3], BCKL [9] and BK [10], represented as uncertainty bands illustrating the p_T/M ranges of the used data. Since these results were extracted from prompt-J/ψ cross sections, neglecting ψ(2S) and χ_c feed-down, we rescaled them by 2/3, the approximate ratio of direct-over-prompt J/ψ yields (a practically p_T/M-independent ratio, given the almost universal p_T/M scaling of the cross sections).

Remarkably, the three results follow a trend seemingly determined by the lower p_T/M limit chosen for the input data, which also reflects the highest event population and most constraining data points. That trend is well described by our curve, implicitly showing that all results are conceptually compatible, while clearly revealing that the specific numerical results are somewhat arbitrary and mostly determined by the choice of the starting p_T/M value (or, in our case, by the normalization point in Eq. 7). Our analysis method keeps data and theory disentangled, by using the data to obtain the best possible experimental determinations of global observables, which are consecutively compared to theory. Such comparisons can, thus, be done as a function of kinematics, which is not possible when the theory calculations are intrinsically embedded in the fits.

From the results of the NRQCD 1 and NRQCD 2 fits, where the χ_{c1} and χ_{c2} cross section shapes are freely adjusted to the data with no imposed links to other contributions, we can appreciate the significance of the experimental indication towards identical p_T/M distributions for S- and P-wave states, which in the UAU scenario was a postulate. Indeed, the χ_c shape functions are very similar to the unpolarized term dominating ψ production, as quantified by the compatibility of the β_u, β_{χ_1} and β_{χ_2} values. This also seems to contradict a priori expectations from NRQCD, where χ_1 and χ_2 production should receive a major contribution from the $^3S_1^{[8]}$ term, while the much flatter unpolarized $^1S_0^{[8]}$ term is strongly suppressed for these states. Although this picture could be somewhat modified by the P-wave singlet contributions (which, being negative, cannot be dominant), it is rather straightforward, in NRQCD, to expect flatter p_T/M dependencies for χ_c than for ψ production. To understand the origin of this strong data indication, which might seem surprising given that the χ_c cross sections are measured at relatively low p_T and with comparatively low precision, we repeated the NRQCD 1 fit keeping only one experimental point for each of the two χ_c cross sections (chosen in the middle of the measured range), letting these measurements constrain the feed-down fractions at that point but not the p_T/M shapes. The results for the χ_c cross section shapes remain fairly consistent with (and even steeper than) the unpolarized ψ results: $\beta_u = 3.37 \pm 0.05$, $\beta_p = 2.85 \pm 0.25$, $\beta_{\chi_1} = 3.57 \pm 0.10$, $\beta_{\chi_2} = 3.68 \pm 0.13$. This test reveals that what prevents the χ_c contribution to J/ψ production from having a flatter p_T/M dependence is the strong similarity between the precisely-measured J/ψ and ψ(2S) cross section shapes.

The NRQCD 1 χ_{c1} and χ_{c2} $^3S_1^{[8]} + {}^3P_{1,2}^{[1]}$ SDC combinations shown in Fig. 4 were calculated with Eq. 4, using $K_\chi = 4.13 \pm 0.09$, the uncertainty leading to the difference between the two solid lines. This K_χ value results from the fit of the χ_{c2}/χ_{c1} ratio, correcting the detection acceptances using, this time, the NRQCD 1 χ polarization scenario; the best-fit curve is almost identical to the one shown in Fig. 2 for the unpolarized acceptance scenario. We remind that no complete fragmentation corrections have been calculated for χ production and the available $^3S_1^{[8]}$ corrections have not been used in this case. The comparison seems to confirm the a priori expectation that NRQCD has some difficulties in reproducing χ_c cross sections as steep as the $^1S_0^{[8]}$-dominated J/ψ one, given the much flatter $^3S_1^{[8]}$ SDC. Nevertheless, the negative $^3P_{1,2}^{[1]}$ terms contribute significantly in the direction of a better compatibility with the data. It will be interesting to see if this trend will be perfected by perturbative calculations including fragmentation corrections.

Interestingly, the data-theory comparison improves further in the NRQCD 2 scenario. The $m_c^2\,\mathcal{S}(^3P_J^{[1]}) + K_\chi\,\mathcal{S}(^3S_1^{[8]})$ combina-

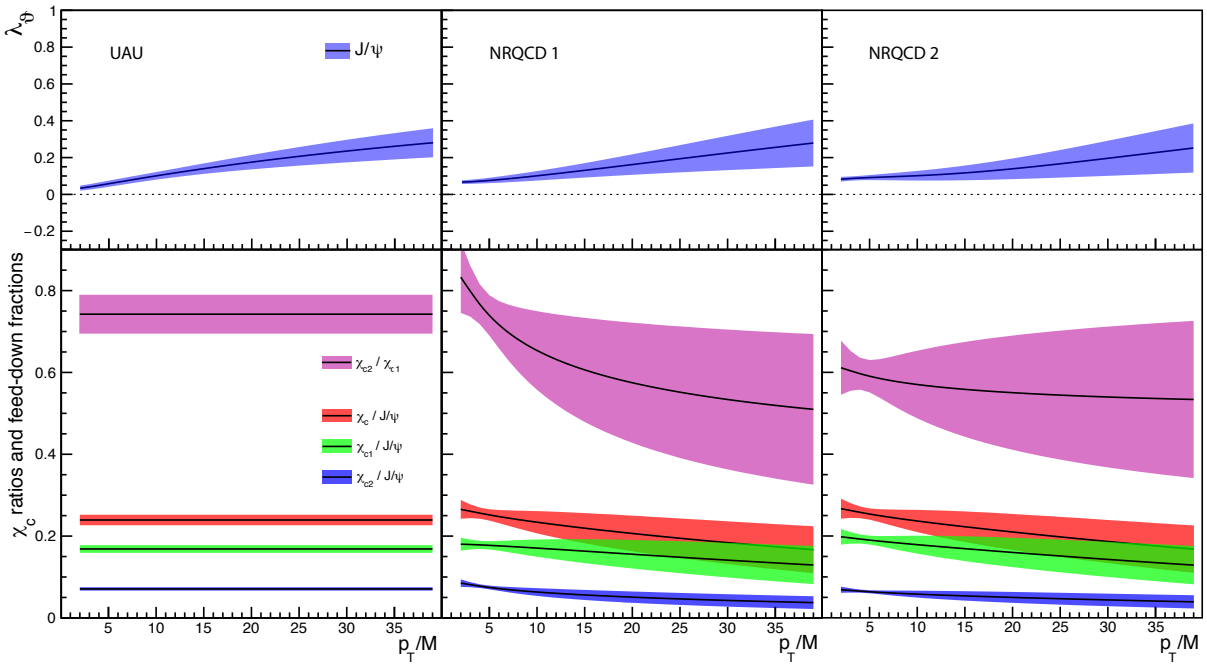

Figure 6: The J/ψ polarization (top) and the χ_{c2}/χ_{c1} ratio and the J/ψ feed-down fractions from χ_{c1}, χ_{c2} and total-χ_c (bottom), in the UAU (left), NRQCD 1 (middle) and NRQCD 2 (right) scenarios. The uncertainty bands reflect correlated variations in the fit parameters.

tions, with K_χ obtained from the χ_2/χ_1 fit assuming the "full" NRQCD χ polarization predictions with singlet terms, approach better the experimental data, as seen in the χ_{c2} cross section (Fig. 4, bottom-right) and in the χ_2/χ_1 fit itself (Fig. 2).

We have seen that the χ_c polarization hypothesis, sole model input to the otherwise fully data-driven scenarios we considered, does not have a crucial influence on the fit results. On the other hand, the NRQCD 2 option brings the seemingly complex theoretical framework closer to a good description of what, at first sight, is an almost universal production picture. Almost ironically, however, the NRQCD 2 polarization hypothesis would represent, if confirmed experimentally, the only case of strong quarkonium polarizations observed by high-p_T experiments and the only evidence for a diversity in the production mechanisms of different states.

Another surprising coincidence is that the sum of the χ_{c1} and χ_{c2} polarizations, weighted by their contributions to the J/ψ polarization (Fig. 3, pink band), is equally small and flat in the NRQCD 2 scenario, as in the NRQCD 1 option (justifying that both models give very similar fit results). This fortuity prevents that the existence of such strong polarizations is observable in the indirect J/ψ production. Even precise measurements of the difference between the J/ψ and ψ(2S) polarizations, or χ_c measurements not resolving the $J = 1$ and 2 states because of poor mass resolution, will not provide enlightening information on the possible individual peculiarities of the P-wave polarizations.

Given these considerations, we argue that χ_{c1} and χ_{c2} polarizations, measured individually, represent a distinctive experimental signature of NRQCD. Fortunately, the almost maximal difference in their predicted values, when singlet contributions are taken into account, facilitates a conclusive experimental test. In particular, the observable $\lambda_\vartheta(\chi_2) - \lambda_\vartheta(\chi_1)$, also shown in Fig. 3 (orange band), is almost immune to systematic uncertainties, like acceptance and efficiency determinations, and can be measured with maximal significance and accuracy.

Figure 6 shows how the J/ψ polarization, χ_{c2}/χ_{c1} ratio and J/ψ feed-down fractions from χ_{c1}, χ_{c2} and total-χ_c extrapolate from the current experimental trends to higher p_T/M, in the χ production scenarios we discussed. These are the observables that, together with the χ polarizations, are in more pressing need of improved measurements by the LHC experiments.

3. Discussion and conclusions

The results presented in this Letter should be seen as a complement to the study shown in our previous publication [2], which also provides an extensive motivation and more details on the data used and on the analysis methodology. That paper is devoted to a phenomenological study, exclusively based on empirical functions derived directly from the measured patterns, complemented by one data-inspired hypothesis: all charmonia are born from a universal production mechanism (UAU), independently of the mass and quantum numbers of the state.

In the present Letter we went beyond the full universality hypothesis, allowing differences between the χ_c production mechanisms and those of the J/ψ and ψ(2S) S-wave mesons. We considered two different models of χ_c production, NRQCD 1 and NRQCD 2, both possibly accommodating the NRQCD hierarchies of processes, with two degrees of complexity in the assumed χ_c polarization ingredients. It is important to emphasise that reasonably precise χ_c polarization measurements, once available, will free the procedure from the necessity of model assumptions, presently imposed by the incomplete picture of quarkonium production provided by the LHC experiments.

The two main questions addressed in this work are: 1) how different and experimentally recognizable are the χ_c production mechanisms from those of the J/ψ and ψ(2S) mesons? 2) and how important will be, for the understanding of quarkonium production, new or improved χ_c measurements?

A first interesting point to mention is that, according to the data, the differential cross sections of the χ_c mesons, as a function of p_T/M, cannot have a significantly different slope with respect to those of the S-wave mesons, given the fact that the measured J/ψ and ψ(2S) spectra are almost identical and knowing that around 25% of the J/ψ yield results from χ_c feed-down decays, which are absent in the ψ(2S) case. The significance of this finding can be quantified by comparing the χ_c vs. J/ψ shape differences allowed by the measured data with the typical shape variations between the component subprocesses foreseen by theory. The bottom panel of Fig. 6 shows rather flat shapes for the χ_c-to-J/ψ feed-down fraction (red bands), in all considered scenarios, the small non-flatness representing the maximal shape differences allowed by the data. The shapes of the SDCs, instead, are significantly more different. For example, the ratio between the $^1S_0^{[8]}$ SDC, the dominating term for ψ production, and the $^3S_1^{[8]}$ SDC, the only octet term contributing to χ production, changes by more than a factor of 10 from low to high p_T/M, as seen in the left panel of Fig. 1 (green curve).

The questions mentioned above were not addressed quantitatively in Ref. [2]; in the UAU scenario χ_c production is assumed, by construction, to be kinematically indistinguishable from ψ production. Moreover, while being a simple and natural conjecture, almost a mirror of the seemingly universal production scenario shown by the data, that model contradicts both the v-scaling rules and the HQSS relations, which constitute important ingredients of the NRQCD framework. Therefore, to address those questions and to investigate how well the data patterns can be accounted for in NRQCD, we freed the χ_c cross sections from any imposed link to the ψ ones (and between themselves), replacing the constraint of universal production with hypothetical χ_c polarizations. To evaluate the dependence of the results on this model ingredient, we used two options, both inspired by NRQCD calculations.

The first variant (NRQCD 1) assumes small and flat χ_1 and χ_2 polarizations, as if, as an outcome of improved calculations, the unphysical and wildly varying singlet contributions converged to the physical and smooth $^3S_1^{[8]}$ term, which they already closely resemble for $p_T/M > 10$ (Fig. 1, right panel). The second variant (NRQCD 2) can be considered as the state-of-the-art NRQCD scenario, where we inject χ_1 and χ_2 polarizations properly determined from a previous fit of the χ_{c2}/χ_{c1} ratio, using current SDC calculations. Such polarizations happen to be opposite in sign and almost maximal at low p_T/M, potentially representing an experimental smoking-gun signature. This analysis leads, in both the NRQCD 1 and NRQCD 2 cases, to scenarios that are, apart from the χ_c polarizations, essentially identical to the UAU option, with the χ_{c1}, χ_{c2} and ψ mesons having approximately the same p_T/M shapes. We conclude that the "universal solution" is a strong indication of the data, independently of specific χ_c polarization hypotheses.

Given the absence of experimental observations differentiating the production kinematics of any particular state, the variety of p_T/M behaviours of the processes foreseen in NRQCD for the different S- and P-wave states, as seen in Fig. 1, seems excessive and unnatural. And yet, comparing the experimental bands obtained for ψ, χ_{c1} and χ_{c2} cross sections with the corresponding "NRQCD shapes", calculated as suitable SDC combinations, leads to a surprising observation. Despite the initial impression of unnecessary complexity, the NRQCD calculations can come close to reproducing the uniformity of the p_T/M trends and the lack of polarization seen in the data, thanks to unexpectedly effective cancellations of heterogeneous process contributions.

The fact that NRQCD manages to mimic a scenario of almost universal and unpolarized production can be explained as the result of four simultaneous "coincidences".

1. The sum of the polarized processes contributing to ψ production is much smaller than the unpolarized term, irrespectively of p_T/M. In the NRQCD language, this means that the sum $^3S_1^{[8]} + {}^3P_J^{[8]}$ is small with respect to the $^1S_0^{[8]}$ term. Our current results tend to indicate that the $^3S_1^{[8]}$ and, especially, the $^3P_J^{[8]}$ terms are individually small, but the present level of uncertainties prevent us from probing the idea that, as predicted by v-scaling rules, the $^1S_0^{[8]}$, $^3S_1^{[8]}$ and $^3P_J^{[8]}$ terms have comparable magnitudes and that the smallness of the $^3S_1^{[8]} + {}^3P_J^{[8]}$ sum follows an internal cancellation, made possible by the fact that the $^3P_J^{[8]}$ and $^3S_1^{[8]}$ SDCs have opposite signs and rather similar shapes, for $p_T/M > 5$ (Fig. 1). More precise measurements of the J/ψ and ψ(2S) polarizations will presumably validate one of the two scenarios: a λ_ϑ almost independent of p_T/M would favour the hypothesis that the two terms cancel each other, while a continuously changing λ_ϑ would suggest that both have small, but not identical, magnitudes.

2. While the $^3S_1^{[8]}$ and $^1S_0^{[8]}$ SDCs have remarkably different slopes (Fig. 1), adding the negative $^3P_1^{[1]}$ SDC to the $^3S_1^{[8]}$ term results in a χ_{c1} cross section shape almost identical to the $^1S_0^{[8]}$ term (Fig. 4, bottom left).

3. Also the $^3S_1^{[8]} + {}^3P_2^{[1]}$ sum, constituting the observable χ_{c2} cross section, becomes almost identical to the $^1S_0^{[8]}$ shape (Fig. 4, bottom right). This happens independently of the previous observation, given that the $^3P_1^{[1]}$ and $^3P_2^{[1]}$ shapes (for $p_T/M < 5$) are different (Fig. 1). It is true that HQSS relates the $^3P_1^{[1]}$ and $^3P_2^{[1]}$ LDMEs, as well as the $^3S_1^{[8]} \to \chi_{c1}$ and $^3S_1^{[8]} \to \chi_{c2}$ LDMEs, so that the mixing parameter K_χ, ratio of the P- and S-wave LDMEs, is the same for χ_{c1} and χ_{c2} (Eq. 4). At present, however, the relative proportion of the $^3P_{1,2}^{[1]}$ and $^3S_1^{[8]}$ terms is always considered as a "free" parameter of the theory; the literature does not explicitly mention a relation between the $^3P_1^{[1]}$ and $^3P_2^{[1]}$ SDCs, matching the one between the LDMEs and eventually leading to almost identical χ_{c1} and χ_{c2} observable cross-section shapes. If such a relation existed, it would fix the mixing parameter K_χ and, hence, the $^3S_1^{[8]}$ LDMEs, eliminating this coincidence.

4. The χ_{c1} and χ_{c2} polarizations, also determined by the same $^3P_{1,2}^{[1]} + {}^3S_1^{[8]}$ mixing parameter K_χ and approaching extreme

physical values towards low p_T/M (+1 and −3/5, respectively), become almost unobservable when summed together, weighted by their respective J/ψ feed-down fractions (Fig. 3, purple band in the bottom panel). The surprisingly small and flat polarization resulting from this weighted sum would explain why no manifestations of strong polarized signals have been detected by experiments. Only measurements of J/ψ polarizations discriminating the two individual χ_c feed-down contributions from direct J/ψ production will be able to test this prediction.

Cancellations, especially when their practical realization is entrusted to the fine tuning of free parameters, are fragile and unstable occurrences, requiring very precise ingredients. Further improvements in the perturbative calculations, especially for the P-wave SDCs, crucial players in this game of coincidences, are needed for more conclusive statements.

Most importantly, χ_{c1} and χ_{c2} polarization measurements have the potential to disclose the true heart of NRQCD, according to which different and strongly polarized individual contributions should be observable, at least in certain processes and/or specific phase-space corners. The existence of such a hidden world of diversified and polarized processes would be brought to light in a spectacular way by the measurement of a large difference (of order 1) between the χ_{c2} and χ_{c1} polarizations (Fig. 3, orange band in the bottom panel), a result that should be achievable with good experimental accuracy, thanks to the cancellation of most systematic effects.

The opportunity provided by such a sensitive observable places NRQCD at a crossroads: should, instead, very similar and weak χ_{c1} and χ_{c2} polarizations be found (as, for example, in the UAU and NRQCD 1 scenarios), the occurrence of fortunate cancellations could probably no longer be advocated. It may still be possible that improved P-wave SDC calculations (e.g., fragmentation corrections have not yet been studied for χ_c singlet production) would rectify the χ_{c1} and χ_{c2} polarization predictions (e.g., in line with the NRQCD 1 conjecture), bringing them close to the measured values and uniforming them to the semi-unpolarized context of quarkonium production. However, this circumstance should be seen as an even more important challenge to NRQCD: it would become an inescapable philosophical necessity to wonder whether the homogeneity of the observed kinematic patterns deserves a more natural theoretical explanation than a conspiracy of coincidences.

Acknowledgements

We are indebted to Hua-Sheng Shao, who kindly gave us the NLO calculations of the short distance coefficients. The work of P.F. is supported by FCT, Portugal, through the grant SFRH/BPD/98595/2013, while the work of I.K. is supported by FWF, Austria, through the grant P 28411-N36.

References

References

[1] G. T. Bodwin, E. Braaten, P. Lepage, Rigorous QCD analysis of inclusive annihilation and production of heavy quarkonium, Phys. Rev. D51 (1995) 1125, [Erratum: Phys. Rev.D55,5853(1997)]. arXiv:hep-ph/9407339, doi:10.1103/PhysRevD.55.5853,10.1103/PhysRevD.51.1125.

[2] P. Faccioli, M. Araújo, V. Knünz, I. Krätschmer, C. Lourenço, J. Seixas, Quarkonium production at the LHC: a phenomenological analysis of surprisingly simple data patterns, Submitted to Phys. Lett. B. arXiv:XXX.YYY.

[3] K.-T. Chao, Y.-Q. Ma, H.-S. Shao, K. Wang, Y.-J. Zhang, J/ψ polarization at hadron colliders in nonrelativistic QCD, Phys. Rev. Lett. 108 (2012) 242004. arXiv:1201.2675, doi:10.1103/PhysRevLett.108.242004.

[4] H.-S. Shao, Y.-Q. Ma, K. Wang, K.-T. Chao, Polarizations of χ_{c1} and χ_{c2} in prompt production at the LHC, Phys. Rev. Lett. 112 (2014) 182003. arXiv:1402.2913, doi:10.1103/PhysRevLett.112.182003.

[5] H.-S. Shao, HELAC-Onia 2.0: an upgraded matrix-element and event generator for heavy quarkonium physics, Comput. Phys. Commun. 198 (2016) 238. arXiv:1507.03435, doi:10.1016/j.cpc.2015.09.011.

[6] P. Faccioli, C. Lourenço, J. Seixas, H. Wöhri, Determination of χ_c and χ_b polarizations from dilepton angular distributions in radiative decays, Phys. Rev. D83 (2011) 096001. arXiv:1103.4882, doi:10.1103/PhysRevD.83.096001.

[7] G. Aad, et al., Measurement of χ_{c1} and χ_{c2} production with $\sqrt{s} = 7$ TeV pp collisions at ATLAS, JHEP 07 (2014) 154. arXiv:1404.7035, doi:10.1007/JHEP07(2014)154.

[8] S. Chatrchyan, et al., Measurement of the relative prompt production rate of χ_{c2} and χ_{c1} in pp collisions at $\sqrt{s} = 7$ TeV, Eur. Phys. J. C72 (2012) 2251. arXiv:1210.0875, doi:10.1140/epjc/s10052-012-2251-3.

[9] G. T. Bodwin, H. S. Chung, U.-R. Kim, J. Lee, Fragmentation contributions to J/ψ production at the Tevatron and the LHC, Phys. Rev. Lett. 113 (2014) 022001. arXiv:1403.3612, doi:10.1103/PhysRevLett.113.022001.

[10] M. Butenschön, B. A. Kniehl, World data of J/ψ production consolidate NRQCD factorization at NLO, Phys. Rev. D84 (2011) 051501. arXiv:1105.0820, doi:10.1103/PhysRevD.84.051501.